Mutations in *COX7B* Cause Microphthalmia with Linear Skin Lesions, an Unconventional Mitochondrial Disease

Alessia Indrieri,[1] Vanessa Alexandra van Rahden,[2] Valeria Tiranti,[3] Manuela Morleo,[1] Daniela Iaconis,[1] Roberta Tammaro,[1] Ilaria D'Amato,[3] Ivan Conte,[1] Isabelle Maystadt,[4] Stephanie Demuth,[5] Alex Zvulunov,[6] Kerstin Kutsche,[2] Massimo Zeviani,[3] and Brunella Franco[1,7,*]

Microphthalmia with linear skin lesions (MLS) is an X-linked dominant male-lethal disorder associated with mutations in holocytochrome *c*-type synthase (*HCCS*), which encodes a crucial player of the mitochondrial respiratory chain (MRC). Unlike other mitochondrial diseases, MLS is characterized by a well-recognizable neurodevelopmental phenotype. Interestingly, not all clinically diagnosed MLS cases have mutations in *HCCS,* thus suggesting genetic heterogeneity for this disorder. Among the possible candidates, we analyzed the X-linked *COX7B* and found deleterious de novo mutations in two simplex cases and a nonsense mutation, which segregates with the disease, in a familial case. *COX7B* encodes a poorly characterized structural subunit of cytochrome c oxidase (COX), the MRC complex IV. We demonstrated that COX7B is indispensable for COX assembly, COX activity, and mitochondrial respiration. Downregulation of the *COX7B* ortholog (*cox7B*) in medaka (*Oryzias latipes*) resulted in microcephaly and microphthalmia that recapitulated the MLS phenotype and demonstrated an essential function of complex IV activity in vertebrate CNS development. Our results indicate an evolutionary conserved role of the MRC complexes III and IV for the proper development of the CNS in vertebrates and uncover a group of mitochondrial diseases hallmarked by a developmental phenotype.

Mitochondria are key players in crucial cellular functions that include oxidative metabolism, ion homeostasis, signal transduction, and programmed cell death. When dysfunctional, mitochondria can contribute to the pathogenesis of a variety of human diseases, such as cancer, neurodegeneration, and aging.[1,2]

Mitochondrial disorders are associated with abnormalities of the common final pathway of mitochondrial energy metabolism, i.e., oxidative phosphorylation (OXPHOS). Their clinical manifestations are extremely heterogeneous and range from lesions of single tissues or structures, such as the optic nerve in Leber's hereditary optic neuropathy (LHON [MIM 535000) or the cochlea in maternally inherited nonsyndromic deafness (MIM 50008), to more widespread lesions, including myopathies, encephalomyopathies, cardiopathies, or complex multisystem syndromes. The age of onset for these diseases ranges from neonatal to adult life.[3,4]

Microphthalmia with linear skin lesions (MLS [MIM 309801]) is an X-linked dominant male-lethal neurodevelopmental disorder due to mutations in holocytochrome *c*-type synthase (*HCCS* [MIM 30056]).[5] Impaired HCCS function in yeast and mice results in OXPHOS defects, supporting a crucial role for HCCS in the formation and function of the mitochondrial respiratory chain (MRC).[6,7]

MLS-affected females exhibit microphthalmia and distinctive linear skin defects usually limited to the face and neck with areas of aplastic skin, which heals to form hyperpigmented lesions. Additional features include facial dysmorphisms, sclerocornea, corneal opacities, agenesis of the corpus callosum, ventriculomegaly, microcephaly, intellectual disability, infantile seizures, and cardiac anomalies. The clinical manifestations vary among affected individuals. Although most of the affected females present with the classical phenotype, a significant number display only a subset of features: some show the typical skin defects without ocular abnormalities, and others display eye abnormalities without skin defects[8] (also see GeneReviews in Web Resources). The majority of affected individuals display monosomy of the Xp22.3 region, where *HCCS* is located. Interestingly, there is no correlation between the phenotype and the extent of the deletion.[9] Several authors have suggested that tissue-specific differentially skewed inactivation of the X chromosome could play a critical role in the development of MLS (reviewed in Van den Veyver,[10] Franco and Ballabio,[11] and Morleo and Franco[12]), in the intrafamilial variability, and in the clinical differences observed among simplex cases. An example of intrafamilial variability is represented by an affected female who only presented with the typical skin defects and who had an affected female fetus with anencephaly. The cytogenetic analyses revealed that both mother and fetus had the same Xp22 deletion, one of the largest described to date for MLS.[9]

The salient features of MLS differ from those found in "canonical" mitochondrial diseases that are usually characterized by postnatal organ failure rather than impaired development of multiple organs and systems. MLS

[1]Telethon Institute of Genetics and Medicine, 80131 Naples, Italy; [2]Institut für Humangenetik, Universitätsklinikum Hamburg-Eppendorf, D-20246 Hamburg, Germany; [3]Unit of Molecular Neurogenetics, The Foundation "Carlo Besta" Institute of Neurology, 20126 Milan, Italy; [4]Centre de Genetique Humaine, Institut de Pathologie et de Genetique, 6041 Gosselies (Charleroi), Belgium; [5]Gemeinschaftspraxis für Humangenetik, 99084 Erfurt, Germany; [6]Schneider Children's Medical Center of Israel, Faculty of Health Sciences, Medical School for International Health, Ben-Gurion University of the Negev, 84105 Beer-Sheva, Israel; [7]Medical Genetics Services, Department of Pediatrics, Federico II University, 80131 Naples, Italy
*Correspondence: franco@tigem.it
http://dx.doi.org/10.1016/j.ajhg.2012.09.016.

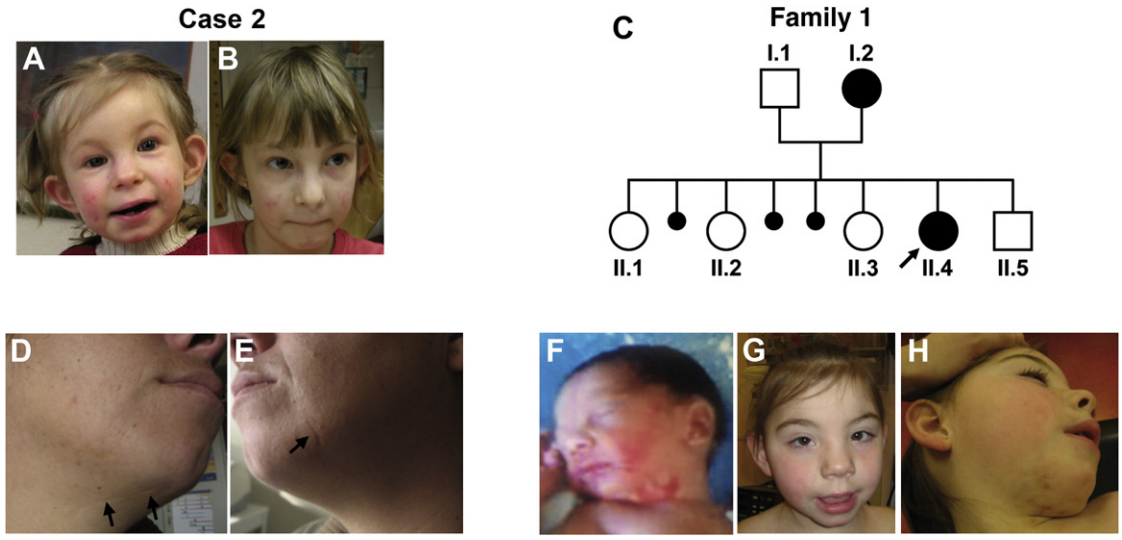

Figure 1. Photographs of Individuals in whom *COX7B* Mutations Were Identified
(A and B) Photographs of case 2 at the ages of 1 year and 10 months (A) and 7 years (B). She had an asymmetric face with limited eyelid closure and linear skin defects (which became less obvious with age) on the face and neck.
(C) Pedigree of family 1. Proband II.4 is the fourth child of healthy and unrelated parents. The couple has three healthy daughters, II.1, II.2, and II.3, and one healthy son, II.5. Three pregnancies ended with spontaneous abortions of unknown sex early in the first trimester.
(D–H) Photographs of individual II.4 (F–H) and her mother (I.2). At birth, individual I.2 presented with linear skin defects, which healed with scaring (arrows in D and E). Individual II.4 had facial dysmorphism with telecanthus, long upslanting palpebral fissures, a short nose, mild retrognathia, and posteriorly rotated ears (G). Linear and patchy erythroderma is located on the cheeks and neck; it was more pronounced at birth (F) than at the age of 5 years (H).

represents a remarkable example of a truly developmental phenotype associated with mitochondrial dysfunction. Moreover, the skin involvement in mitochondrial diseases is atypical and can include hirsutism and hypertrichosis as described in Leigh syndrome (MIM 256000) and twisted hairs as reported in Bjornstad syndrome (MIM 262000).[13]

HCCS is highly conserved throughout evolution from fungi to metazoan and catalyzes the incorporation of heme moieties on both cytochrome (Cyt) c_1, an integral component of MRC complex (C) III, and Cytc, the mitochondrial CIII–CIV electron shuttle.[14,15] A few clinically diagnosed MLS cases in whom no mutations in *HCCS* could be found have been identified[16,17] (B.F. and K.K., unpublished results), thus suggesting genetic heterogeneity for this disorder. In all these cases, analysis of the methylation pattern revealed 100% skewing of X chromosome inactivation in peripheral-blood cells (data not shown).

We postulated that mutations affecting other components of CIII–CIV could lead to the MLS phenotype. Cytochrome c oxidase (COX), a fundamental MRC complex (CIV), in humans comprises three mitochondrial-encoded proteins (COX1, COX2, and COX3) that assemble with ten nuclear-encoded proteins (COX4, COX5A, COX5B, COX6A, COX6B, COX6C, COX7A, COX7B, COX7C, and COX8) to form the mature holocomplex.[18–21] Because of the expected X-linked inheritance pattern, we selected, among possible candidates, the only X-linked gene, *COX7B* (MIM 603792), which encodes a small and poorly characterized subunit of CIV.[22,23] We then analyzed 14 available MLS-affected females in whom mutational analysis failed to detect mutations in *HCCS*, and we found three mutations in *COX7B*.

Case 1 is the first child of unrelated Jewish parents. She was born at term and displayed linear skin lesions on the neck and face at birth. Her mother had had two previous spontaneous abortions of unknown sex during the first trimester of pregnancy. This individual presented with facial dysmorphisms, short stature, microcephaly, and poor growth. Eye examination was normal and showed neither microphthalmia nor visual impairment. Her psychomotor development was normal. A full description of this case is available.[24] Fluorescent in situ hybridization (FISH) studies excluded deletion and translocation of the Xp22 region.

Case 2 was born at term from nonconsanguineous parents. She presented with poor growth, microcephaly, multiple linear skin defects on the face and neck, an asymmetric face with limited eyelid closure, a small chin, and a right clumped foot. A right diaphragmatic hernia was surgically corrected. A cranial ultrasound revealed a thin corpus callosum. No ocular abnormalities were detected. An echocardiogram showed ventricular hypertrophy, pulmonary hypertension, and a small atrial septal defect. She also had left renal agenesis and ureteral duplication of the right kidney. During a follow-up examination, she showed short stature. Linear skin defects healed over time, although they were still evident on the cheeks and chin (Figures 1A and 1B). She had mild psychomotor delay and learning difficulties. Routine cytogenetic analysis revealed a normal female karyotype. FISH studies excluded deletion and translocation of the Xp22 region.

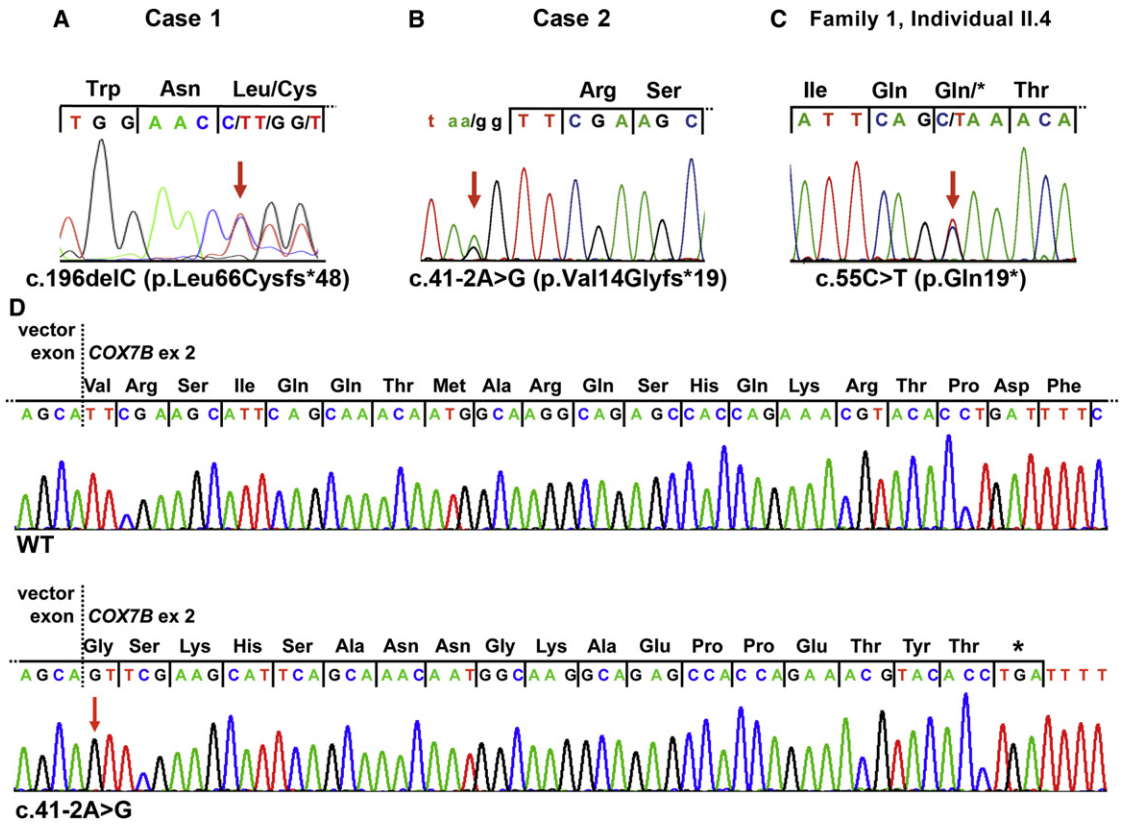

Figure 2. ***COX7B*** **Mutations in Individuals with MLS**
(A) Sequence electropherograms from genomic DNA of case 1. She was found to be heterozygous for a de novo 1 bp deletion (leading to a frameshift) in exon 3 of *COX7B*.
(B) Sequence electropherograms from genomic DNA of case 2. She was found to be heterozygous for a de novo splice site mutation, c.41-2A>G, in intron 1.
(C) Sequence electropherograms from genomic DNA of individual II.4 from family 1. The heterozygous mutation c.55C>T (p.Gln19*) in exon 2 was found in individuals II.4 and I.2.
(D) Sequence electropherograms of *COX7B* transcripts obtained from a minigene assay. Representative sequences of a transcript (containing the spliced exon 2 of *COX7B*) obtained from the WT construct is shown on the top, whereas one representative transcript obtained from the minigene with the c.41-2A>G mutation is shown on the bottom. Mutant (c.41-2G) *COX7B* transcripts result in a truncated COX7B (p.Val14Glyfs*19). Nucleotide triplets and encoded amino acids are indicated.

In family 1, proband II.4 is the fourth child of unrelated individuals. Before she was born, her mother, individual I.2, had three pregnancies that ended with spontaneous abortions of unknown sex within the first trimester (Figure 1C). At birth, individual I.2 presented with linear skin defects, which became less obvious with age (Figures 1D and 1E). She has mild myopia and normal cognitive functions. Proband II.4 was born at 30 weeks of gestation with a normal birth weight and microcephaly. She presented with linear and patchy erythroderma (more evident at birth) on the cheeks and neck (Figures 1F and 1H), facial dysmorphisms (including telecanthus, arched eyebrows, long upslanting palpebral fissures, a short nose, mild retrognathia, and posteriorly rotated ears) (Figure 1G), and tetralogy of Fallot. She also had an asymmetric thorax with widely spaced nipples, bilateral clinodactyly of the fifth fingers, and a bilateral sandal gap. She developed intellectual disabilities and was diagnosed with attention-deficit/hyperactivity disorder at 4 years of age. When she was 3 months old, brain magnetic resonance imaging showed delayed myelination. She had poor vision, and an ophthalmologic examination revealed pale optic discs and altered visual-evoked potentials. Array-comparative-genomic-hybridization analysis (Agilent 44K) in II.4 revealed a 387 kb microduplication of unknown clinical significance on 12p13.33 and excluded a deletion of the Xp22 region. This microduplication was also present in her healthy father.

Individuals enrolled in this study were collected under the approval of the ethics committee responsible for each center, and informed consent was obtained from subjects or their legal representatives.

COX7B (RefSeq accession number NM_001866.2) is localized to the Xq21.1 region, comprises three coding exons, and encodes an 80 amino acid mitochondrial protein. Using specific primers listed in Table S1 (available online), we sequenced the coding region and exon-intron boundaries of *COX7B* in the above-described cases. In case 1, this analysis led to the identification of a heterozygous 1 bp deletion, c.196delC (leading to a frameshift), in exon 3 of *COX7B* (Figure 2A). This mutation most likely

Table 1. Clinical Features Reported in MLS-Affected Individuals Carrying Deletions or Point Mutations in *HCCS* or Point Mutations in *COX7B*

	HCCS Deletions or Point Mutations[a]	*COX7B* Point Mutations			
				Family 1	
Clinical Features	**Occurrence**	**Case 1**	**Case 2**	**II.4**	**I.2**
Microphthalmia	43/55 (78%)	–	–	–	–
Sclerocornea	22/55 (40%)	–	–	–	–
Other eye abnormalities	28/55 (51%)	–	–	+[b]	–
Linear skin lesions	42/55 (76%)	+	+	+	+
Nail dystrophy	3/55 (5%)	+	–	–	–
Microcephaly, agenesis of the corpus callosum, and other CNS abnormalities	24/52 (43%)	+	+	+	–
Intellectual disability	9/42 (21%)	–	+	+	–
Short stature	16/36 (44%)	+	+	–	–
Cardiac abnormalities	21/52 (40%)	–	+	+	–
Diaphragmatic hernia	3/55 (5%)	–	+	–	–
Genitourinary abnormalities	14/55 (25%)	–	+	–	–

Please note that for each feature listed in the table, the total number of individuals taken into account includes only cases in whom each clinical feature was analyzed and documented.
[a]See GeneReviews in Web Resources, as well as Sharma et al.,[8] Kono et al.,[26] and Zumwalt et al.[27]
[b]Pale optic discs and altered visual-evoked potentials.

leads to the generation of a COOH-terminal truncated COX7B with 46 novel amino acids (p.Leu66Cysfs*48). The resulting mutant protein is predicted to lack the domain that interacts with the two COX subunits, namely COX4 and COX6C.[22] The mutation was absent in the parents (paternity confirmed) and in 200 ethnically matched controls (data not shown).

In case 2, *COX7B* sequence analysis revealed the presence of a heterozygous splice mutation (c.41-2A>G) in intron 1 (Figure 2B). The mutation was absent in the parents. This mutation is predicted to create in intron 1 a novel splice acceptor site one base before the wild-type (WT) splice site. In vitro analysis of the c.41-2A>G change was performed by the Exon Trapping System (GIBCO Invitrogen). A 2,705 bp genomic fragment that encompasses intron 1, exon 2, and intron 2 of *COX7B* for both WT and mutant sequences was cloned into vector pSPL3, sequenced for integrity, and transfected into COS-7 cells. We analyzed ten WT (c.41-2A) and ten mutant (c.41-2G) *COX7B* transcripts. In all transcripts obtained from the WT minigene, we identified a normal sequence (Figure 2D). In contrast, 90% of the mutated transcripts contained an additional guanine at the beginning of exon 2; this addition led to out-of-frame transcripts and most likely to the formation of a truncated COX7B with 18 novel amino acids at the COOH-terminal region (p.Val14Glyfs*19) (Figure 2D).

Finally, we also identified a heterozygous nonsense mutation (c.55C>T [p.Gln19*]) in the second exon of *COX7B* in individual II.4 (Figure 2C). The mutation was identified in both individual II.4 and her mother (I.2), whereas the three healthy sisters (II.1, II.2, and II.3) of individual II.4 and her healthy brother (II.5) inherited the WT *COX7B* allele from their mother (Figure 1C). This mutation might result either in a functional null allele as a result of nonsense-mediated mRNA decay (NMD) or in a COX7B lacking a large COOH-terminal portion (Δaa19–80). The latter assumption is more likely given that mRNAs with a premature termination codon located within 50–55 nt upstream of the most 3′ exon-exon junction are generally not targeted for NMD.[25]

None of the nucleotide changes were present in the available databases (dbSNP or the National Heart, Lung, and Blood Institute [NHLBI] Exome Variant Server). All together, our results clearly indicate that mutations in *COX7B* cause MLS. Table 1 illustrates the clinical features observed in individuals with deletions or point mutations in *HCCS* and those observed in individuals with point mutations in *COX7B*. Some of the individuals in whom no mutation in either *COX7B* or *HCCS* could be identified might bear small deletions not identified in the present study. It is also possible that mutations in other MRC-associated genes will possibly explain these cases.

The function of COX7B within CIV is still unknown. To investigate this issue, we silenced *COX7B* in HeLa cells by using ON-TARGET siRNA (Dharmacon) against human *COX7B* and ON-TARGET Non-Targeting siRNA (Dharmacon) to a final concentration of 50 nM. Measured by quantitative real-time PCR, the degree of *COX7B* silencing in siRNA-treated HeLa cells ($HeLa^{COX7B}$) was >50% higher than the levels detected in HeLa cells incubated only with the transfection reagent ($HeLa^{WT}$) and HeLa cells transfected with nontargeting siRNA ($HeLa^{C}$) (Figure S1).

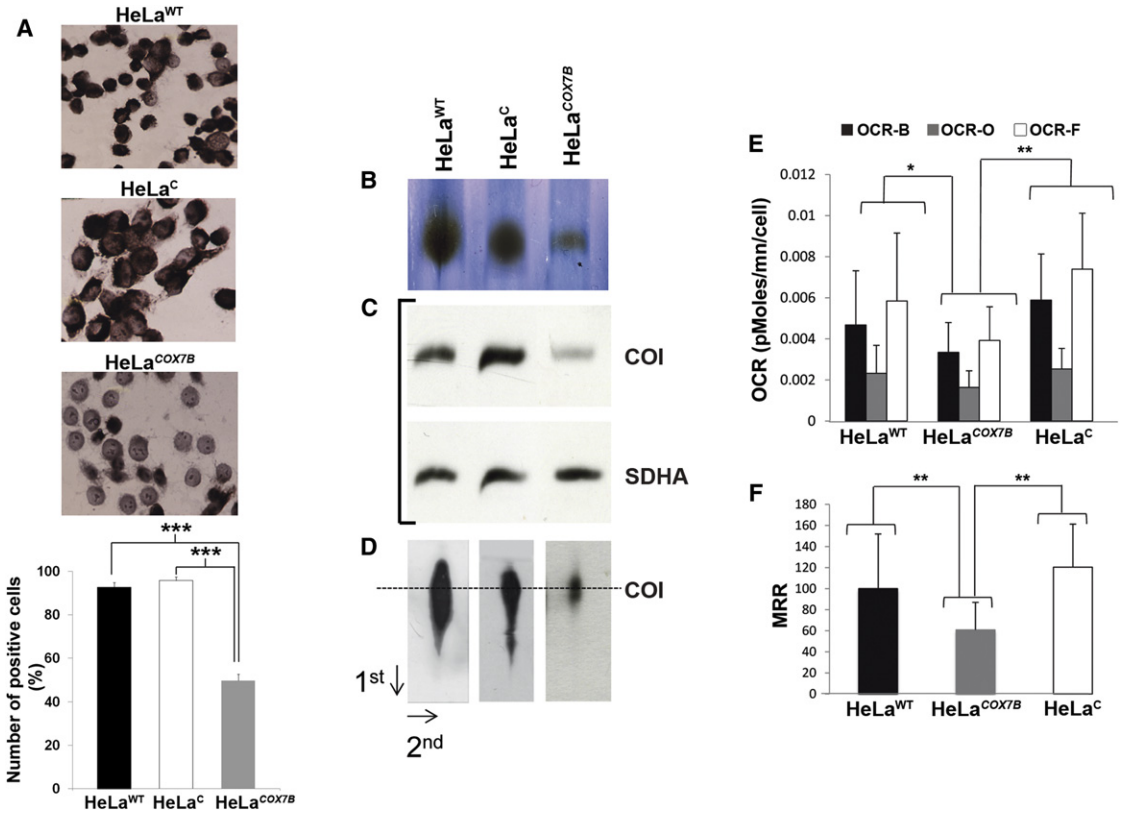

Figure 3. COX7B Is Necessary for CIV Activity, Assembly, and MRC Functioning
(A) COX histochemical reactions in HeLa^{WT}, HeLa^{C}, and HeLa^{COX7B} cells; note the marked reduction in HeLa^{COX7B} cells compared to controls. The bottom panel shows the number of COX-positive cells in each sample.
(B) In-gel activity of CIV on 1D-BNGE in the same cells. 1D-BNGE was performed on mitochondria isolated from HeLa cells as described.[29] COX-specific in-gel activity was visualized on 100 μg of protein (for each sample) run through 1D-BNGE as described.[30] The intensity of the COX-specific band was markedly reduced in HeLa^{COX7B} lysate.
(C) 1D-BNGE immunoblot analysis of mitochondria immune visualized with antibodies against COI and against the 70 kDa (SDHA) CII subunit used as a control.
(D) Immunodetection of CIV assembly intermediates on two-dimensional BNGE immunoblot shows marked decrease in the steady-state level of CIV holoenzyme detected by the COI antibody in HeLa^{COX7B} cells. The amount of loaded samples is the same as in (C).
(E) The OCR was measured by microscale oxygraphy in different conditions as described in Invernizzi et al.[31] The resulting OCR profile in HeLa^{WT}, HeLa^{COX7B}, and HeLa^{C} cells was normalized to cell number.
(F) Analysis of the MRR in HeLa^{WT}, HeLa^{COX7B}, and HeLa^{C} cells. MRR was calculated by the subtraction of the rotenone-insensitive OCR from OCR-F (OCR after FCCP addition). Error bars represent the standard deviation; *$p < 0.05$, **$p < 0.01$, ***$p < 0.001$ in an unpaired, two-tailed Student's t test.

We first carried out a COX-specific histochemical reaction[28] that showed markedly reduced signal in HeLa^{COX7B} cells compared to both HeLa^{WT} and HeLa^{C} cells (Figure 3A). We then measured in-gel COX activity on mitochondrial extracts from HeLa^{WT}, HeLa^{C}, and HeLa^{COX7B} cells (extracts were separated by one-dimensional blue-native gel electrophoresis [1D-BNGE]). The COX-specific reactive band was markedly reduced in the HeLa^{COX7B} extract, in striking contrast with the robust reaction detected in both HeLa^{WT} and HeLa^{C} extracts (Figure 3B). Holo-COX immunodetection by immunoblot analysis on 1D-BNGE with anti-COX subunit I (COI) antibodies showed marked reduction of the fully assembled COX in HeLa^{COX7B} cells as compared to HeLa^{WT} and HeLa^{C} samples (Figure 3C). Likewise, immunoblot analysis on two-dimensional BNGE showed that COI cross-reacting material was present at the position corresponding to the fully assembled COX in HeLa^{WT} and HeLa^{C} samples, whereas it was hardly detectable in HeLa^{COX7B} samples insomuch that it prevented the visualization of any possible subassembly intermediate (Figure 3D).

We also analyzed the oxygen-consumption rate (OCR) in living cells by using microscale oxygraphy (XF96 Seahorse) according to described protocols.[31] The OCR was measured in basal conditions (OCR-B) in the presence of the CV inhibitor oligomycin (OCR-O), corresponding to respiration state 4, and in the presence of the OXPHOS uncoupler FCCP (OCR-F), corresponding to respiration state 3.[31,32] Values were significantly lower in HeLa^{COX7B} cells than in HeLa^{WT} and HeLa^{C} cells (Figure 3E); as a consequence, the maximal respiration rate (MRR), an index of the functional reserve of mitochondrial respiration that is obtained by the subtraction of OCR-B from OCR-F,[31,32] was also reduced (Figure 3F). These results demonstrate

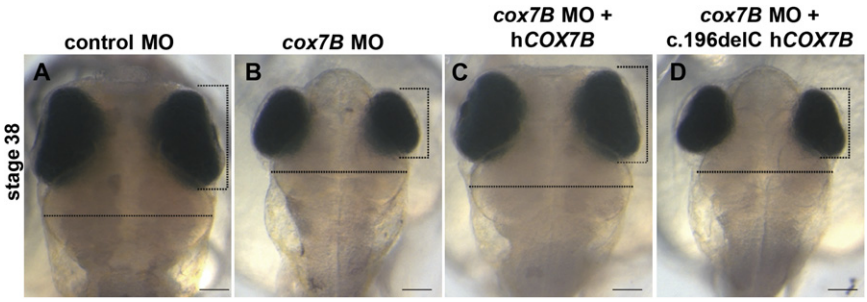

Figure 4. *cox7B* Downregulation In Vivo Mimics MLS

Bright-field dorsal views of embryos injected with a control MO (A), *cox7B* MO (B), *cox7B* MO + h*COX7B* mRNA (C), *cox7B* MO + c.196delC-h*COX7B* mRNA (D) at stage 38. The injection of the *cox7B* MO induced microphthalmia (vertical dashed line in B) and microcephaly (horizontal dashed line in B). The overexpression of h*COX7B* mRNA fully rescued microphthalmia and microcephaly (vertical and horizontal dashed lines in C), induced by MOs showing the specificity of the morphant phenotype. No amelioration of the phenotype was observed in embryos coinjected with *cox7B* MO + c.196delC-h*COX7B* mRNA, indicating that this mutation impairs COX7B activity (D). Scale bars represent 100 μm. MOs (Gene Tools) were injected into fertilized embryos at the 1- to 2-cell stage. mRNA sequences corresponding to WT h*COX7B* and c.196delC h*COX7B* were obtained with the SP6 mMessage mMachine kit (Ambion). Rescue experiments were performed by coinjection of WT h*COX7B* and c.196delC h*COX7B* with the *cox7B* MO into one blastomere of the embryos at the 1- to 2-cell stage. eGFP mRNA was always included in the injection solutions as a reporter.

that the COX7B subunit is necessary for COX activity, COX assembly, and mitochondrial respiration.

Finally, to evaluate the role of COX7B in vivo, we downregulated *cox7B* in medakafish (*Oryzias latipes*) by using a morpholino (MO)-based knockdown approach. We identified the medaka *COX7B* ortholog (*cox7B*) by screening available genomic sequences by using the human and murine COX7B sequences (RefSeq NP_001857.1 and NP_079655.1, respectively). The entire *cox7B* coding sequence, including part of the 5′ UTR, was isolated by reverse-transcriptase-PCR amplification from cDNA derived from a pool of medaka embryos at different stages (data not shown). The medaka *cox7B* transcript (HE717026) encodes a 78 amino acid protein with 51% identity to the human COX7B. We designed a specific MO against the second splice acceptor site (*cox7B* MO) and injected it into embryos at the 1- to 2-cell stage. Embryos injected with a mutated form of the MO (control MO) were used as controls. The efficiency and specificity of MOs (Gene Tools) were verified with the recommended controls[33] (Figure S2 and Tables S1 and S2).

The *cox7B* morphants showed a dose-dependent phenotype characterized by microcephaly and microphthalmia (Figures 4A and 4B and Table S2). The presence of microphthalmia after *cox7B* downregulation demonstrates that COX7B plays a role in eye development. Therefore, the lack of microphthalmia in the cases analyzed (Table 1) might be explained by a selective pattern of X inactivation in those individuals.[11,12] The identification of additional cases with *COX7B* mutations will be crucial for clarifying this issue. Morphant embryos also displayed cardiovascular abnormalities with evident pericardial edema and formation of an unlooped heart (Figure S3). Interestingly, two of the cases with *COX7B* point mutations presented with cardiac abnormalities. These defects, which are similar to those observed in *hccs* morphants (B.F., unpublished data), were progressive and led to death at the hatching stage. Injection of morphants with human (h) *COX7B* mRNA rescued the phenotype (Figure 4C and Table S2), demonstrating that COX7B function is important for proper development and is conserved among vertebrates. On the contrary, injection of c.196delC h*COX7B* did not rescue the phenotype, indicating that this mutation impairs COX7B activity (Figure 4D and Table S2).

In summary, our results indicate that severe impairment of the MRC's terminal segment, which funnels all the reducing equivalents from both $NADH^{+}H^{+}$ and $FADH_2$ electron donors to O_2, causes a severe developmental phenotype, which is an uncommon feature in canonical mitochondrial disorders. Interestingly, mutations in nuclear-encoded subunits of CIII–CIV are exceptionally rare in humans. To date, a single homozygous missense mutation in the nuclear *COX6B1* (MIM 124089), encoding a COX subunit, has been reported in an individual with mitochondrial encephalomyopathy (COX deficiency [MIM 220110]).[34]

HCCS and *COX7B* are both ubiquitously expressed (data available at BIOGPS database) given that they are required for cellular respiration. However, the phenotypic manifestations observed in MLS-affected females mainly affect the CNS and other specific organs, suggesting that dosage and function of these proteins are critical for selected tissues. It is possible that differential tissue sensitivity to mitochondrial ATP depletion (high versus low energy demand) and/or overproduction of reactive oxygen species might elicit different molecular responses in the absence of HCCS or COX7B in selected tissue types and might therefore induce the blockage of cell replication and/or an increased cell death.[1,35,36]

Deregulation in these processes and X chromosome inactivation could concur to select OXPHOS-proficient cells in HCCS- and COX7B-depleted tissues, thus attenuating or abolishing MRC defects in the surviving tissues and individuals. Both *HCCS* and *COX7B* are subjected to X inactivation. Interestingly, X-linked genes show variable patterns of inactivation and are expressed to different extents from some inactive X chromosomes, suggesting a remarkable degree of expression heterogeneity among females.[37]

The molecular basis of many inherited developmental disorders that involve the CNS still remains to be

determined. On the basis of our results, MRC-related genes might very well underlie lethal and so far unrecognized developmental disorders and should be considered as possible candidates for these conditions.

All together, our results indicate an essential role for MRC function in correct CNS development and uncover the existence of a group of mitochondrial diseases in which impairment of the CIII–CIV MRC segment results in developmental defects.

Supplemental Data

Supplemental Data include three figures and two tables and can be found with this article online at http://www.cell.com/AJHG.

Acknowledgments

This work was supported by the Pierfranco and Luisa Mariani Foundation Italy, the Italian Telethon Foundation (GGP11011 and GPP10005), CARIPLO grant 2011/0526, and the Italian Association of Mitochondrial Disease Patients and Families (Mitocon) (to M.Z.) and the Deutsche Forschungsgemeinschaft (KU 1240/6-1 to K.K.). B.F. is also supported by the Italian Telethon Foundation. We thank Sandro Banfi, Nicola Brunetti-Pierri, and Graciana Diez-Roux for critical reading of the manuscript and helpful discussion. We also thank Francesco Salierno and Inka Jantke for excellent technical assistance.

Received: July 26, 2012
Revised: August 31, 2012
Accepted: September 28, 2012
Published online: November 1, 2012

Web Resources

The URLs for data presented herein are as follows:

BioGPS, http://biogps.org/#goto=welcome
dbSNP, http://www.ncbi.nlm.nih.gov/SNP/
EMBL Nucleotide Sequence Database, http://www.ebi.ac.uk/embl/
NHLBI Exome Sequencing Project Exome Variant Server, http://snp.gs.washington.edu/EVS/
GeneReviews, Morleo, M., and Franco, B. (2009). Microphthalmia with Linear Skin Defects Syndrome, http://www.ncbi.nlm.nih.gov/books/NBK7041
Online Mendelian Inheritance in Man (OMIM), http://www.omim.org/

Accession Numbers

The EMBL Nucleotide Sequence Database accession number for the medaka *cox7B* sequence reported in this paper is HE717026.

References

1. Wallace, D.C. (2005). A mitochondrial paradigm of metabolic and degenerative diseases, aging, and cancer: A dawn for evolutionary medicine. Annu. Rev. Genet. *39*, 359–407.
2. Shadel, G.S. (2008). Expression and maintenance of mitochondrial DNA: New insights into human disease pathology. Am. J. Pathol. *172*, 1445–1456.
3. Zeviani, M., and Di Donato, S. (2004). Mitochondrial disorders. Brain *127*, 2153–2172.
4. Schapira, A.H. (2012). Mitochondrial diseases. Lancet *379*, 1825–1834.
5. Wimplinger, I., Morleo, M., Rosenberger, G., Iaconis, D., Orth, U., Meinecke, P., Lerer, I., Ballabio, A., Gal, A., Franco, B., and Kutsche, K. (2006). Mutations of the mitochondrial holocytochrome c-type synthase in X-linked dominant microphthalmia with linear skin defects syndrome. Am. J. Hum. Genet. *79*, 878–889.
6. Drenckhahn, J.D., Schwarz, Q.P., Gray, S., Laskowski, A., Kiriazis, H., Ming, Z., Harvey, R.P., Du, X.J., Thorburn, D.R., and Cox, T.C. (2008). Compensatory growth of healthy cardiac cells in the presence of diseased cells restores tissue homeostasis during heart development. Dev. Cell *15*, 521–533.
7. Dumont, M.E., Ernst, J.F., Hampsey, D.M., and Sherman, F. (1987). Identification and sequence of the gene encoding cytochrome c heme lyase in the yeast Saccharomyces cerevisiae. EMBO J. *6*, 235–241.
8. Sharma, V.M., Ruiz de Luzuriaga, A.M., Waggoner, D., Greenwald, M., and Stein, S.L. (2008). Microphthalmia with linear skin defects: A case report and review. Pediatr. Dermatol. *25*, 548–552.
9. Lindsay, E.A., Grillo, A., Ferrero, G.B., Roth, E.J., Magenis, E., Grompe, M., Hultén, M., Gould, C., Baldini, A., Zoghbi, H.Y., et al. (1994). Microphthalmia with linear skin defects (MLS) syndrome: Clinical, cytogenetic, and molecular characterization. Am. J. Med. Genet. *49*, 229–234.
10. Van den Veyver, I.B. (2001). Skewed X inactivation in X-linked disorders. Semin. Reprod. Med. *19*, 183–191.
11. Franco, B., and Ballabio, A. (2006). X-inactivation and human disease: X-linked dominant male-lethal disorders. Curr. Opin. Genet. Dev. *16*, 254–259.
12. Morleo, M., and Franco, B. (2008). Dosage compensation of the mammalian X chromosome influences the phenotypic variability of X-linked dominant male-lethal disorders. J. Med. Genet. *45*, 401–408.
13. Birch-Machin, M.A. (2000). Mitochondria and skin disease. Clin. Exp. Dermatol. *25*, 141–146.
14. Schaefer, L., Ballabio, A., and Zoghbi, H.Y. (1996). Cloning and characterization of a putative human holocytochrome c-type synthetase gene (HCCS) isolated from the critical region for microphthalmia with linear skin defects (MLS). Genomics *34*, 166–172.
15. Schwarz, Q.P., and Cox, T.C. (2002). Complementation of a yeast CYC3 deficiency identifies an X-linked mammalian activator of apocytochrome c. Genomics *79*, 51–57.
16. Morleo, M., Pramparo, T., Perone, L., Gregato, G., Le Caignec, C., Mueller, R.F., Ogata, T., Raas-Rothschild, A., de Blois, M.C., Wilson, L.C., et al. (2005). Microphthalmia with linear skin defects (MLS) syndrome: Clinical, cytogenetic, and molecular characterization of 11 cases. Am. J. Med. Genet. A. *137*, 190–198.
17. García-Rabasco, A., De-Unamuno, B., Martínez, F., Febrer-Bosch, I., and Alegre-de-Miquel, V. (2012). Microphthalmia with Linear Skin Defects Syndrome. Pediatr. Dermatol. Published online May 21, 2012. http://dx.doi.org/10.1111/j.1525-1470.2012.01735.x.
18. Carr, H.S., and Winge, D.R. (2003). Assembly of cytochrome c oxidase within the mitochondrion. Acc. Chem. Res. *36*, 309–316.
19. Fontanesi, F., Soto, I.C., Horn, D., and Barrientos, A. (2006). Assembly of mitochondrial cytochrome c-oxidase,

a complicated and highly regulated cellular process. Am. J. Physiol. Cell Physiol. *291*, C1129–C1147.
20. Herrmann, J.M., and Funes, S. (2005). Biogenesis of cytochrome oxidase-sophisticated assembly lines in the mitochondrial inner membrane. Gene *354*, 43–52.
21. Mick, D.U., Fox, T.D., and Rehling, P. (2011). Inventory control: Cytochrome c oxidase assembly regulates mitochondrial translation. Nat. Rev. Mol. Cell Biol. *12*, 14–20.
22. Tsukihara, T., Aoyama, H., Yamashita, E., Tomizaki, T., Yamaguchi, H., Shinzawa-Itoh, K., Nakashima, R., Yaono, R., and Yoshikawa, S. (1996). The whole structure of the 13-subunit oxidized cytochrome c oxidase at 2.8 A. Science *272*, 1136–1144.
23. Fornuskova, D., Stiburek, L., Wenchich, L., Vinsova, K., Hansikova, H., and Zeman, J. (2010). Novel insights into the assembly and function of human nuclear-encoded cytochrome c oxidase subunits 4, 5a, 6a, 7a and 7b. Biochem. J. *428*, 363–374.
24. Zvulunov, A., Kachko, L., Manor, E., Shinwell, E., and Carmi, R. (1998). Reticulolinear aplasia cutis congenita of the face and neck: A distinctive cutaneous manifestation in several syndromes linked to Xp22. Br. J. Dermatol. *138*, 1046–1052.
25. Nagy, E., and Maquat, L.E. (1998). A rule for termination-codon position within intron-containing genes: When nonsense affects RNA abundance. Trends Biochem. Sci. *23*, 198–199.
26. Kono, T., Migita, T., Koyama, S., and Seki, I. (1999). Another observation of microphthalmia in an XX male: Microphthalmia with linear skin defects syndrome without linear skin lesions. J. Hum. Genet. *44*, 63–68.
27. Zumwalt, J., Moorhead, C., and Golkar, L. (2012). Fourteen-month-old girl with facial skin thinning. Pediatr. Dermatol. *29*, 217–218.
28. Tiranti, V., Munaro, M., Sandonà, D., Lamantea, E., Rimoldi, M., DiDonato, S., Bisson, R., and Zeviani, M. (1995). Nuclear DNA origin of cytochrome c oxidase deficiency in Leigh's syndrome: Genetic evidence based on patient's-derived rho degrees transformants. Hum. Mol. Genet. *4*, 2017–2023.
29. Nijtmans, L.G., Henderson, N.S., and Holt, I.J. (2002). Blue Native electrophoresis to study mitochondrial and other protein complexes. Methods *26*, 327–334.
30. Zerbetto, E., Vergani, L., and Dabbeni-Sala, F. (1997). Quantification of muscle mitochondrial oxidative phosphorylation enzymes via histochemical staining of blue native polyacrylamide gels. Electrophoresis *18*, 2059–2064.
31. Invernizzi, F., D'Amato, I., Jensen, P.B., Ravaglia, S., Zeviani, M., and Tiranti, V. (2012). Microscale oxygraphy reveals OXPHOS impairment in MRC mutant cells. Mitochondrion *12*, 328–335.
32. Brand, M.D., and Nicholls, D.G. (2011). Assessing mitochondrial dysfunction in cells. Biochem. J. *435*, 297–312.
33. Eisen, J.S., and Smith, J.C. (2008). Controlling morpholino experiments: Don't stop making antisense. Development *135*, 1735–1743.
34. Massa, V., Fernandez-Vizarra, E., Alshahwan, S., Bakhsh, E., Goffrini, P., Ferrero, I., Mereghetti, P., D'Adamo, P., Gasparini, P., and Zeviani, M. (2008). Severe infantile encephalomyopathy caused by a mutation in COX6B1, a nucleus-encoded subunit of cytochrome c oxidase. Am. J. Hum. Genet. *82*, 1281–1289.
35. Nunnari, J., and Suomalainen, A. (2012). Mitochondria: In sickness and in health. Cell *148*, 1145–1159.
36. Hamanaka, R.B., and Chandel, N.S. (2010). Mitochondrial reactive oxygen species regulate cellular signaling and dictate biological outcomes. Trends Biochem. Sci. *35*, 505–513.
37. Carrel, L., and Willard, H.F. (2005). X-inactivation profile reveals extensive variability in X-linked gene expression in females. Nature *434*, 400–404.